Preparation of mixed matrix PES-based nanofiltration membrane filled with PANI-co-MWCNT composite nanoparticles

Ehsan Bagheripour, Abdolreza Moghadassi[†], and Sayed Mohsen Hosseini

Department of Chemical Engineering, Faculty of Engineering, Arak University, Arak 38156-8-8349, Iran
(*Received 18 June 2015 • accepted 26 November 2015*)

Abstract−Mixed matrix polyethersulfone/PANI-co-MWCNTs composite nanoparticle nanofiltration membrane was prepared by casting solution technique. Polyvinylpyrrolidone was also used as membrane pore former in membrane fabrication. The effect of polyaniline-co-multi walled carbon nanotubes composite nanoparticle concentration in the casting solution on membrane structure and performance was investigated. Scanning optical microscopy and scanning electron microscopy, FTIR analysis, porosity, mean pore size, contact angle, water content, NaCl/Na$_2$SO$_4$ rejection, water flux, tensile strength measurements and 3D surface image were also carried out in membrane characterization. SOM images showed nanoparticle agglomeration at high additive loading ratio. SEM images showed the membrane sub-layer porosity and thickness were changed by use of nanoparticles in membrane matrix. The membrane water content, porosity and pore size were increased by increase of nanoparticle concentration, except for 1%wt. Use of PANI-co-MWCNT nanoparticles in the membrane matrix caused a decrease of membrane contact angle from 63.43 to 46.76°. Salt rejection and water flux were improved initially by increase of nanoparticle concentration up to 0.1%wt and then decreased by more additive concentration. In addition, the membranes tensile strength was reduced by increase of PANI-co-MWCNTs composite nanoparticle concentration. 3D surface images showed a smoother surface for mixed matrix membrane filled with 0.1 wt% PANI-co-MWCNTs. Modified membrane containing 0.1 wt% composite nanoparticles showed better performance compared to others.

Keywords: Nanofiltration, Membrane Fabrication/Characterization, Mixed Matrix, Polyaniline-co-multi Walled Carbon Nanotubes Composite Nanoparticles

INTRODUCTION

One of the most important concerns of governments is how to provide clean water for agriculture, human consumption, industries and energy production. Human survival essentially depends on fresh water, which is increasingly becoming scarce [1-3]. During the last decades, wide-ranging studies on desalination using high-chemical-stability, high-salt-rejection nanofiltration membranes have been done [4]. Development of nanofiltration technology in separation processes is being greatly studied. The NF process has been used in many applications such as waste water reclamation, industrial water production, water softening and in the separation of compounds having different molecular weights [5-10]. Different materials can be used for membrane fabrication, such as metals, ceramics, graphite, glass, and polymers. Most commercially available nanofiltration membranes are made of polymer. All polymers can be used as a barrier or membrane materials, but their chemical and physical properties specifications have reduced their application [11]. Organic polymer has many advantages, such as extensive sources, convenient manufacture, low cost, and easy to achieve the industrialization, but it also has to overcome bad thermostability, weak anti-fouling and poor anti-swelling etc. There are some extensive polymers such as cellulose acetate (CA), polysulfone

(PSf), polyacrylonitrile (PAN), polyvinylidenedifluoride (PVDF), polyetherimide (PEI) and polyethersulfone (PES) which could be used for fabrication nanofiltration and ultrafiltration membranes by phase inversion method [12-15].

Extensive research has already been performed to improve the NF physico-chemical properties which has resulted in various modification techniques. Utilization of different polymeric materials, polymers blending, different additives loading such as nanoparticles and surface modifications are some of the most important techniques for obtaining appropriate membranes [16,17].

Utilizing inorganic nanoparticles or fillers into the polymeric matrixes has also been examined in many applications to enhance the mechanical, thermal and chemical stability of polymeric matrixes in severe conditions, such as high temperature and strongly oxidizing environment and also to improve the separation properties and performance and anti-fouling characteristic of membranes based on synergism between the organic-inorganic component properties [18-21].

PANI-co-MWCNT composite nanoparticle is a well known inorganic nanomaterial which has been of a great interest due to its unique features. PANI is one of the most important and promising intrinsically conducting polymers due to its special features such as easy synthesis, high intrinsic ionic and electronic conductivity, simple acid-base chemistry as well as environmental and thermal stability and relatively low cost. This makes it usable in different separation processes for water and waste water treatment applications [22,23]. Also, polyaniline can remove toxic ions from water

[†]To whom correspondence should be addressed.
E-mail: a.moghadassi@gmail.com, a-moghadassi@araku.ac.ir

due to the existence of the nitrogen atom with lonely electron pair as a reactive adsorption site. It has been revealed that sawdust can efficiently adsorb cadmium ions when it is coated with polyaniline [24,25].

In addition, multiwalled carbon nanotube is also an important and unique nanoparticle containment of specific structural, chemical and mechanical properties because of its high aspect ratio and high surface area, high chemical stability and adsorption capability. Polymeric modification of MWCNT can lead to introduction of new properties such as hydrophilicity, better dispersibility and compatibility with polymers in nanocomposite membranes [26]. CNTs are able to adsorb polymers, coated with and covalently bonded with polymers during a polymerization reaction [26]. New multi-walled carbon nanotubes (MWCNTs) were modified by in situ polymerization of acrylic acid (AA) in aqueous solution in the presence of potassium persulfate (KPS) as initiator and ethylene glycol (EG) as cross-linker to obtain stable grafted polyacrylic acid (PAA) on MWCNTs surface with better performance compared to pure MWCNT nanoparticles [27].

In PANI-co-MWCNT composite nanoparticles, due to the existence of interfacial interaction or the formation of hydrogen bonds between aminate and carboxylic groups of aniline and functionalized multiwalled carbon nanotubes, there is good interaction between both components [22,28].

Lately electrodialysis heterogeneous anion exchange membrane modified by PANI-co-MWCNT composite nanoparticles was prepared and characterized for water treating. But currently no researches have considered incorporation of PANI-co-MWCNT composite nanoparticles into NF membrane. Thus, preparation of mixed matrix NF membranes and investigation the effect of various concentrations of PANI-co-MWCNT composite nanoparticles on their performance and morphology for the application in desalination processes is the main target of current research.

For this purpose, PES/PANI-co-MWCNT composite nanoparticle mixed matrix nanofiltration membrane was prepared by casting solution technique and phase inversion method using DMAC as solvent. PANI-co-MWCNT composite nanoparticle was also employed as composite filler in the membrane fabrication to im-prove the PES NF physico/chemical properties.

Scanning optical microscopy (SOM), scanning electron microscopy (SEM) and FTIR analysis, water content, contact angle, porosity, pore size, NaCl/Na$_2$SO$_4$ salt rejection, water flux, tensile strength measurements and 3D surface image were also used in membrane characterization.

MATERIALS AND METHODS

1. Materials

Polyethersulfone (PES) (Ultrason E6020P, MW=58,000 g/mol, BASF) was used as the membrane base binder. Polyvinylpyrrolidone (PVP) (MW=25,000 g/mol, Merck) was used as a pore former. Polyaniline/multiwalled carbon nanotube composite nanoparticles (PANI/MWCNTs, nanoparticles, particle size=80 nm, including 10 wt% MWCNTs and 90 wt% PANI) were supplied from Nanoradbehan Co., Iran, was used as inorganic filler additive/modifier. N, N-dimethylacetamide (DMAC) (Mw=87.12 g·Mol^{-1}, Merck) and deionized water were used as solvent and non-solvent, respectively. The chemical structure of used PANI-co-MWCNT composite nanoparticles is shown in Table 1.

2. Fabrication of Composite NF Membrane

The nanocomposite membranes were prepared by casting solution technique and phase inversion method. The fabrication was done by dissolving the certain amount of PES (20 wt%) and PVP (1 wt%) into the solvent (DMAC) in glassy reactors by a mechanical stirrer (Model: Velp Scientifica Multi 6 stirrer) for more than 4 hr. This was followed by dispersing PANI/MWCNT composite nanoparticles, with various concentrations, as an additive (nanofiller) in polymeric solutions. For better dispersion of nanoparticles and breaking up their aggregates, the solutions were sonicated for 1 h by an ultrasonic cleaner bath (Parsonic11Smodel, S/N PN-88159, Iran). The obtained homogeneous solutions were cast onto clean and dry glass plates by using a casting knife with constant thickness of 150 μm. Then, they were dipped into deionized water as non-solvent without prior evaporation time. After exchanging solvent and non-solvent and precipitation step, membranes were formed. Then they were kept in new containers with fresh deion-

Table 1. The chemical structure of used PANI-co-MWCNT composite nanoparticles
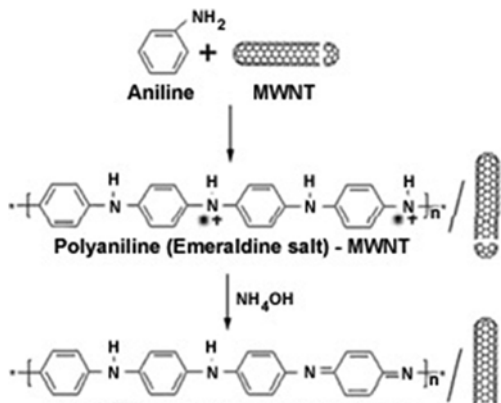
Chemical structure

Polyaniline/multiwalled carbon nano tube composite nanoparticles (PANI/MWCNTs)

Membrane (M_n)	Nanoparticles (PANI/MWCNTs) (%wt)	Solvent (DMAC) (%wt)
M1	0	79
M2	0.01	78.99
M3	0.1	78.9
M4	1	78

[a]Constant concentration of PES and PVP (20 : 1 wt/wt%)

ized water for one day to remove any soluble components in the membrane structures. The membranes were dried between two filter paper sheets at room temperature ($25\pm2\,^{\circ}$C) for one day before using. The composition of used casting solutions is given in Table 2.

3. Membrane Characterization

3-1. Membrane Morphology

3-1-1. Scanning Electron Microscopy (SEM)

For cross-sectional characterization of the fabricated membranes, scanning electron microscopy (SEM) (Seron Technology Inc. Korea) was used. Before examination of prepared membranes by SEM, the membranes were dipped in liquid nitrogen for 5 minutes and after being frozen, they were broken. Then, they were sputtered with gold thin film and scanned with an electron microscope.

3-1-2. Scanning Optical Microscopy (SOM)

For characterization of the surface of the fabricated membranes, scanning optical microscopy (Olympus, Model IX 70, transmission mode with light going through the sample) was used. The membranes were cut into the small sizes and placed between two glass lamellas, then observed by optical microscope.

3-2. FTIR Spectroscopy

FTIR spectra measurements were carried out to analyze the structure and surface chemistry to confirm the existence of PANI-co-MWCNTs composite nanoparticles on membrane structure and surface. FTIR spectra analysis involved the Galaxy Series FTIR 5000 spectrometer.

3-3. Membrane Water Content

Membrane water content is a factor for measuring the hydrophilicity of the membranes [28]. For determining it, a certain weight of membrane pieces was dipped in distilled water for 24 h. Next, the wet membranes quickly were located between two filter paper sheets to remove additional surface water and then were weighed immediately (OHAUS, Pioneer[TM], Readability: 10-4 g, Ohaus Corp.). After being placed in an oven at a fixed temperature ($50\,^{\circ}$C) for 24 hr, they were weighed and the water content percentage was measured as the weight difference between dried and wet membranes. The following equation was used for water content percent [27-30]:

$$\%\text{Water content} = \frac{W_w - W_d}{W_w} \times 100 \tag{1}$$

where W_w and W_d are the wet and dry membranes weight (g), respectively. To minimize measuring errors, all measurements were repeated three times for each sample and then their average values were reported.

3-4. Contact Angle Measurement

To investigate the surface wettability and surface hydrophilicity of PES-PANI-co-MWCNTs NF membranes, the contact angle measurement was employed. Doing so, very small droplets of the deionized water were dropped on the membrane surface in several random places, and the droplets were imaged with a digital camera. The average values of the measurements were reported to minimize errors.

3-5. Porosity and Mean Pore Size Measurements

The overall porosity (ε) was calculated by the expression below [31]:

$$\varepsilon(\%) = \frac{W_w - W_d}{\rho_f V_m} \times 100 \tag{2}$$

where and V_m are water density (g/cm^3) and membrane small size volume (cm^3), respectively. All of the experiments were done three times and the results carried out are mean values to ensure minimizing experimental errors.

The mean pore radius size (rm), based on the pure water flux and porosity data was employed by Guerout-Elford-Ferry equation as follows [32]:

$$r_m = \sqrt{\frac{(2.9 - 1.75\,\text{Porosity})8\eta lQ}{\text{Porosity} * A * \Delta P}} \tag{3}$$

where η is the water viscosity (8.9×10^{-4} Pa·s), l is the membrane thickness (m), Q is the pure water flux (m^3/s), and ΔP is the operating pressure (6 bar).

3-6. Membrane Performance

Capability of fabricated nanofiltration membranes in salts removal from water was investigated in terms of NaCl and Na$_2$SO$_4$ rejection. This experiment was carried out in a dead end cell at 5 bars (Fig. 1). The feed solutions were prepared separately by dissolving 1,000 mg/L salts in deionized water. For salt rejection percentage calculations, the following equation was used:

$$\text{Rejection} \% = 1 - \left(\frac{C_p}{C_f}\right) * 100 \tag{4}$$

where, C_p and C_f are salt concentrations in permeate and feed, respectively [33,34] and were measured by conductivity meter (Ohaus Corporation, S/N B143385306, U.S.A).
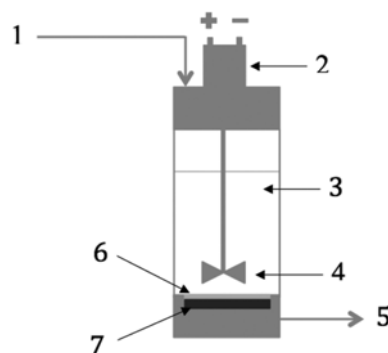

Fig. 1. Schematic diagram of used dead-end stirred cell.

1. N$_2$ gas input	5. Permeate (dilute solution)
2. Electrical motor	6. Membrane
3. Feed solution	7. Supported layer
4. Blades	

The permeation flux was determined by measuring the water passed through the membranes in terms of L/m²h and calculated by below equation [35]. In all, gas nitrogen by purity of 99.9% was used for driving force.

$$Jv=Q/A \, (\Delta t) \tag{5}$$

where Jv is permeation flux (L/m²h), Q is content of permeated water (L), A is membrane area (m²) and Δt is sampling time (h). All experiments were performed at ambient temperature.

3-7. Membrane Mechanical Strength

For characterization of the fabricated nanofiltration membranes mechanical properties, their tensile strength was examined according to ASTM1922-03 [36]. Thus all samples were prepared in the standard sizes and the experiments were done three times to minimize the experimental errors.

3-8. 3D Surface Image

The surface roughness of the prepared mixed matrix membranes was investigated using 3D surface image metrology software.

RESULTS AND DISCUSSION

1. Confirmation of PANI-co-MWCNT Presence in the Membrane Matrix

An FTIR spectrum of mixed PES/PANI-co-MWCNT composite nanoparticles is shown in Fig. 2. For PES/PANI-co-MWCNT matrix,
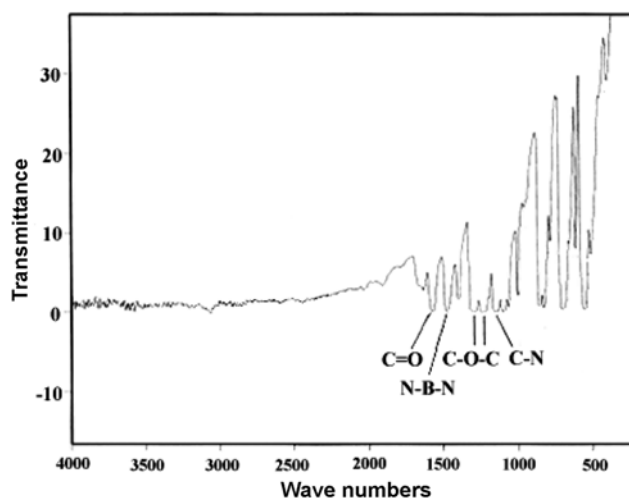

Fig. 2. FTIR spectra analysis of mixed matrix PES/PANI-co-MWCNT membrane.

the characteristic peaks of C=O and C-O-C were observed at 1,600, 1,333, and 1,258 cm⁻¹, confirming the presence of MWCNT in the composite matrix. With respect to FTIR spectra of PES/PANI-co-MWCNT composite, illustrated in this figure, the peaks of C-N at 1,149 and N-B-N at 1,494 cm⁻¹ verify the presence of PANI on the composite structure.
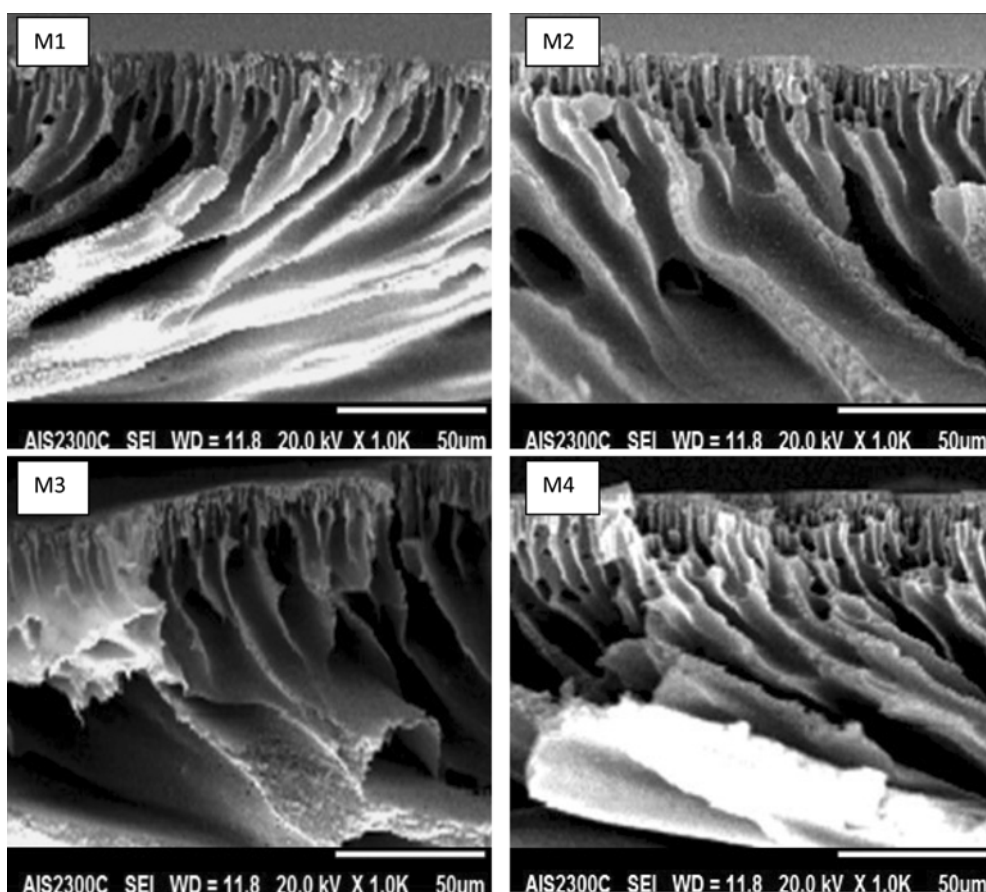

Fig. 3. The cross sectional SEM images of fabricated membranes with different PANI-co-MWCNT composite nanoparticles concentration.

2. Morphological Studies

SEM images (Fig. 3) obviously show changes in the membrane pore shape, porosity and surface thickness during addition various concentration of nanoparticles. According to the SEM images, the porosity obviously has increased in the sub-layer by employment of 0.01 and 0.1%wt nanoparticles compared to the compact structure of pristine PES membrane. In this condition the membrane surface thickness has decreased. This event can be explained by phase inversion rate effect on the membrane structure type as a result of the interaction between casting film and non-solvent. The presence of composite hydrophilic PANI-co-MWCNT in the casting solution increases the rate of solvent/non-solvent exchange during phase inversion process, resulting in reduction of skin-layer thickness with more porosity in the sub-layer (SEM images b, c contain of 0.01 and 0.1%wt nanoparticles) [37]. But increase of nanoparticle concentration to 1%wt inversely increases membrane surface thickness and decreases porosity in the sub-layer (see SEM image d). This can be explained by casting solution viscosity increment at high nanoparticle concentration and its effect on the rate of phase inversion phenomena too. In this situation, coagulation of casting film in nonsolvent drops, leading to the formation of structure with thicker surface and lower porosity in sub-layer [38].

The results calculated by Eqs. (2) and (3) for porosity and mean pore size, respectively, presented in Fig. 4 are another evidence for
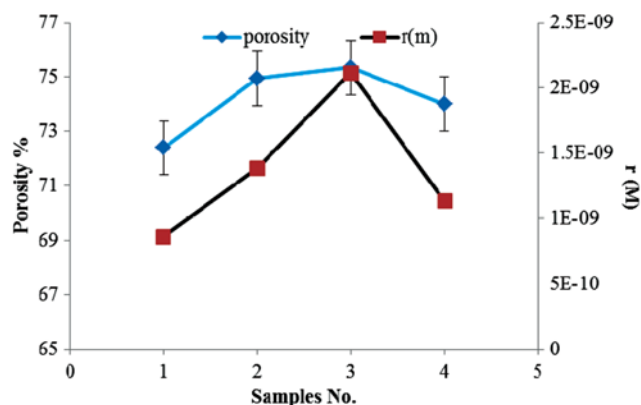

Fig. 4. The effect of PANI-co-MWCNT nanoparticles concentration on porosity and mean pore size.

the above two observations. As seen in this figure, porosity and mean pore radius initially have increased for the prepared membranes by use of PANI-co-MWCNT nanoparticles in the casting solution (0.01 and 0.1%wt), and then they have decreased at 1%wt nanoparticle usage. These observations are in agreement with SEM images b, c, and d in Fig. 3.

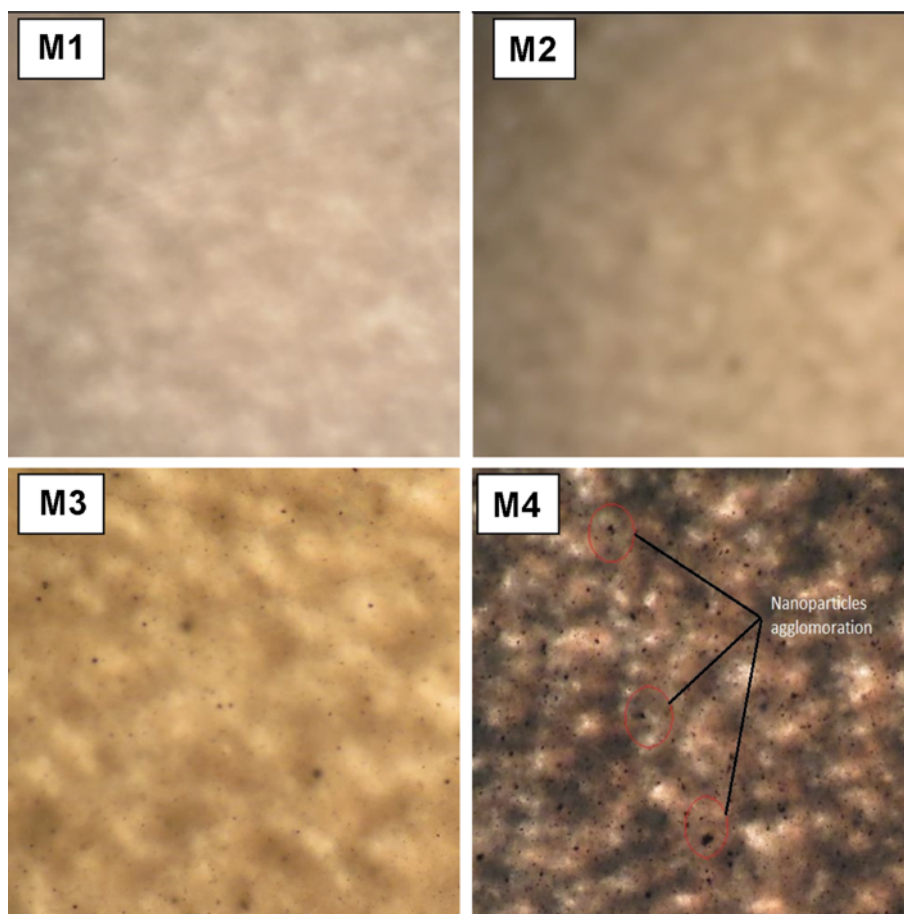SOM images of the fabricated membranes for study on the

Fig. 5. The SOM images (10X magnifications) of prepared membranes with different concentrations of nanoparticles.
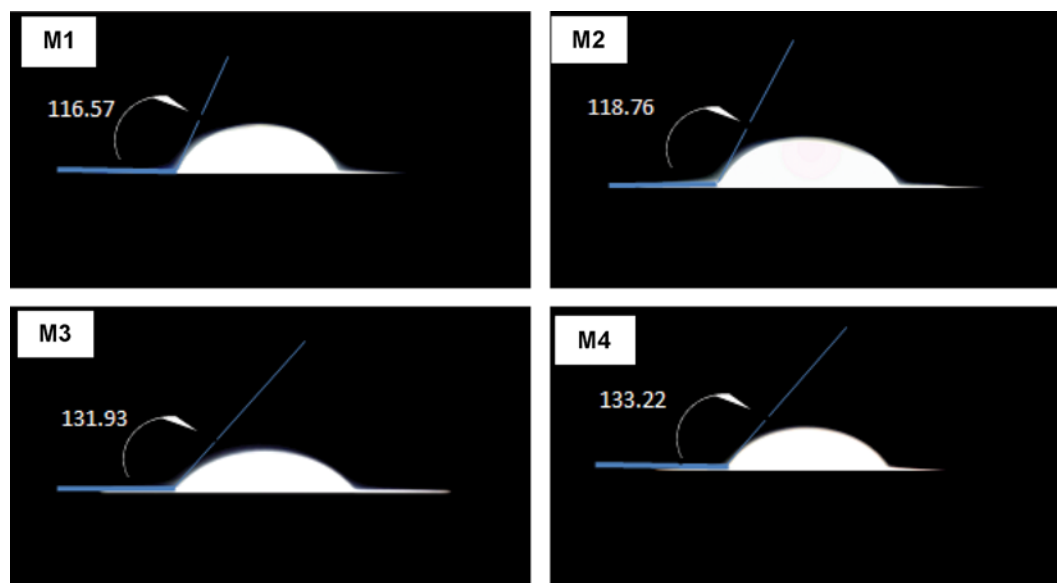
Fig. 6. Contact angle images of composite membranes with different concentration of nanoparticles.

Table 3. The effect of PANI-co-MWCNT concentration on membrane contact angle

Membrane (M_n)	Contact angle (°)
M1	63.43
M2	61.24
M3	48.07
M4	46.76

nanoparticles distribution behavior are given in Fig. 5. The SOM images obviously indicate that nanoparticle agglomeration might occur at high concentrations. In the SOM image d, the nanoparticle agglomeration on high additive concentration was encircled by red lines.

3. Contact Angle and Water Content

To evaluate the hydrophilicity and wettability of bare and mixed PES membranes, a contact angle analysis and water content were used. Fig. 6 shows contact angle images of composite membranes containing different concentration of nanoparticles. According to this figure, whatever composite nanoparticle concentration in the mixed matrix has increased, the angle between the deionized water droplet and membrane surface clearly has decreased. The results for contact angle measurement, given in Table 3, indicate that contact angle decreased from 69.43 to 46.76 without and with nanoparticles (1%wt), respectively. The results indicate that membrane hydrophilicity was improved by the increase in PANI-co-MWCNT composite nanoparticle content employed in the membrane matrix.

In addition, the results obtained (Fig. 7) for water content measured indicated that increase of PANI-co-MWCNT nanoparticle concentration in the casting solution also led to increase in membrane water content. From one point of view, increasing of contact angle and water content may be attributed to the hydrophilic characteristic of PANI-co-MWCNT composite nanoparticles, which improves the membrane hydrophilicity. The movement of hydro-
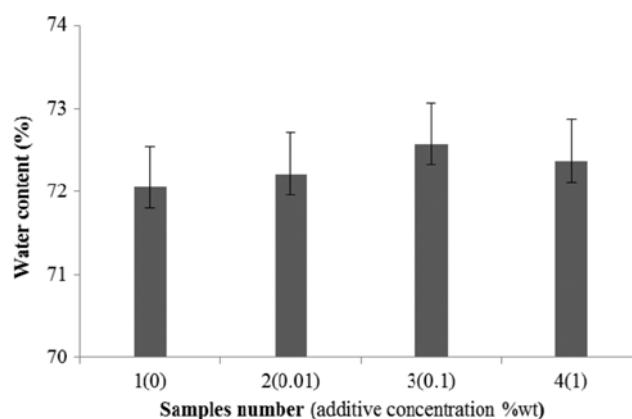

Fig. 7. The effect of PANI-co-MWCNT nanoparticles concentration on membrane water content.

philic composite nanoparticles to the membrane surface (top layer) during phase inversion process increases the membrane surface hydrophilicity. This was confirmed by images of water droplets in the contact with the membrane surface in Fig. 6 and also the results of contact angle measurements presented in Table 3. From another point of view, increasing of water content by increasing of composite nanoparticles can be caused by the porosity and pore size growth (see Fig. 4). In this condition, there are more spaces in the membrane structure for water storing, leading to water content increment. SEM images (Fig. 3) also illustrated greater macrovoids in the membrane sub-layer for the modified membranes containing composite nanoparticles (0.01 and 1%wt), compared to pristine one that confirms more open structure for water storing.

In Fig. 7, by more employment of PANI-co-MWCNT (1%wt) a slight decrease in membrane water content was observed. This reduction of membrane water content at 1%wt nanoparticle loading ratio may be attributed to the pore filling phenomenon by the additional nanoparticles, leading to lower porosity and lower pore

size, which restricts the water molecules accommodation [39]. In fact, by more increasing of nanofiller concentration up to 1%wt, it is possible that voids and cavities in the membrane matrix are surrounded and occupied by the nanoparticles, which results in less water adsorption. The results of porosity and pore size shown in Fig. 4 reflected the same behaviors that confirm this subject. The SEM image, d in Fig. 3, is another evidence for decreasing of water content in this case.

SOM analysis also was used to evaluate the spatial nanoparticle distribution in the membrane matrix. SOM images (Fig. 5) showed uniform distribution of nanoparticles in the membrane matrix at 0.01 and 1%wt nanoparticles loadings relatively. But some nanoparticle agglomeration was observed at high additive concentration (1%wt SOM image, d), which decreases the active surface area of nanoparticles and their effects on the membrane performance and morphology.

Note that measurements were carried out three times for each membrane to minimize experimental errors and their average was reported.

4. Separation Performance of Prepared Membranes

4-1. Salt Rejection

Membrane salt rejection was investigated by using of NaCl (mono-valent) and Na_2SO_4 (bivalent) ionic solutions. The results (Fig. 8) indicated that increase of PANI-co-MWCNT nanoparticle concentration up to 0.1%wt in the casting solution led to increasing of sodium chloride and sodium sulfate rejection for the prepared NF membranes. This may be due to the adsorption characteristic of PANI-co-MWCNT nanoparticles, which caused superior interactions between ions and membrane matrix [40]. The rejection was decreased by increase of PANI-co-MWCNT nanoparticle concentration from 0.1 to 1%wt in the membrane matrix. This can be attributed to nanoparticle agglomeration at high additive concentration (see Fig. 5, SOM image, d), which decreases the amount of adsorptive active sites/active surface area, thereby decreasing salt adsorption capability by composite nanoparticles, leading to increase of ion percolation throughout the membrane matrix. Among the prepared membrane, modified membrane containing 0.1%wt PANI-co-MWCNT composite nanoparticles showed
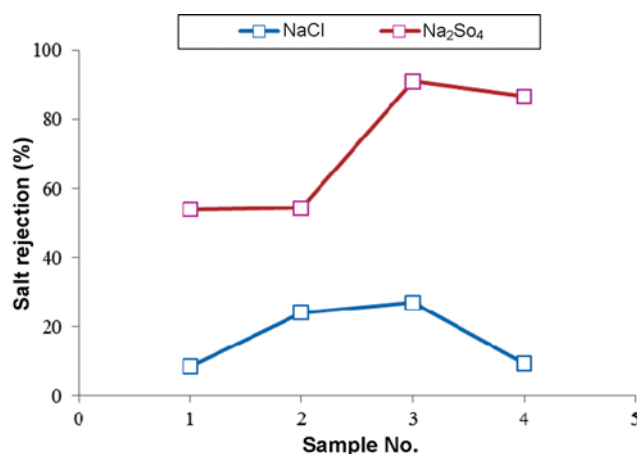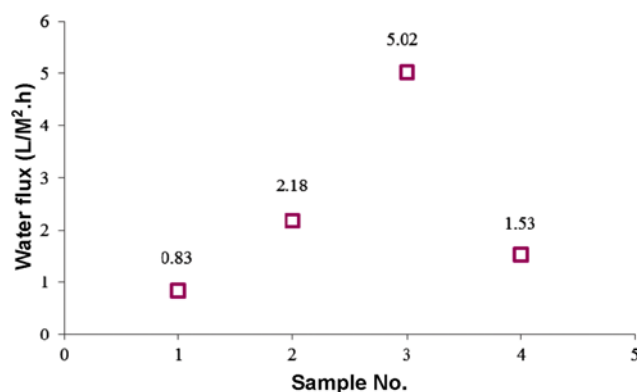

Fig. 9. The effect of PANI-co-MWCNT nanoparticles concentration on membrane water flux.

highest ionic rejection of about 69% and 219% greater than the pristine one for Na_2SO_4 and NaCl salts, respectively.

4-2. Water Flux

The results (Fig. 9) showed that water flux of the prepared mixed matrix membranes was increased sharply by increase of PANI-co-MWCNT nanoparticles up to 0.1%wt in the casting solution. Two major parameters which can influence the membrane permeation flux are membrane hydrophilicity and morphology [41]. It is very well known that increasing of membrane hydrophilicity increases the permeation flux [42]. In addition, the membrane porosity, mean pore size increment and membrane surface thickness reduction are morphological parameters that can improve permeation flux of the membrane too. Thus, the water flux improvement in Fig. 9 partly can be due to increase of membrane water content/hydrophilicity which improves the water flux. Moreover, it is possible that larger pores and macro-voids in the membrane structure and more porosity made by addition of nanoparticles into the casting solution (0.01 and 0.1%wt) (were observed in Figs. 3, and 4), which facilitates the water transportation through the membrane, can be other logical reasons for water flux improvement.

The membrane water flux was decreased by more loading of PANI-co-MWCNT composite nanoparticles from 0.1 to 1%wt in
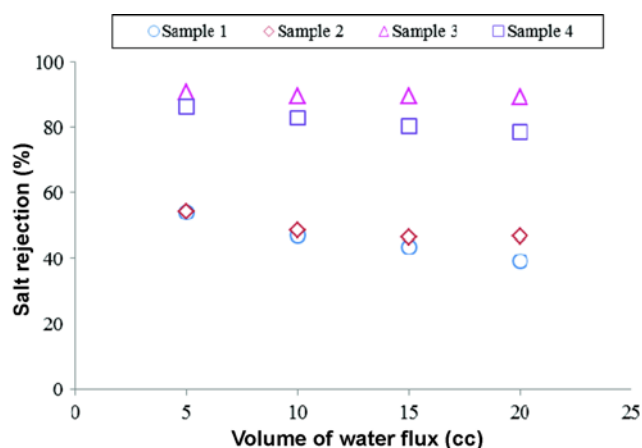

Fig. 8. The effect of PANI-co-MWCNT nanoparticles concentration on membrane rejection (mono and bivalent).

Fig. 10. The membrane Na_2SO_4 rejection versus water permeated flux.

the PES matrix. This may be related to the pore filling/blocking phenomenon at high concentration of nanoparticles, which decreases the water traffic that was explored by others [43,44]. This observation is in very good agreement with SEM and SOM photographs and morphological results demonstrated in Figs. 3 and 4 (SEM image d, porosity and mean pore size) and also with carried out water content measurements presented in Fig. 7. Fig. 10 describes membrane rejection stability against the progress of the separation process. The obtained results revealed that modified membranes containing PANI-co-MWCNT nanoparticles showed more stable rejection compared to pristine ones. Also, the modified membrane containing 0.1%wt composite nanoparticles showed more appropriate performance compared to other modified membrane and pristine ones.

5. Membrane Mechanical Strength

The effect of PANI-co-MWCNT concentration on membrane mechanical properties was examined by membrane tensile strength measurement. The results (Fig. 11) revealed that increase of PANI-co-MWCNT nanoparticle concentration in the casting solution led to decreasing of membrane tensile strength. This is due to increase in amount of voids/cavities (porosity) in membrane matrix by increasing of PANI-co-MWCNT nanoparticle content ratio, which decreases the membrane tensile strength. The increase in transfer channels and porosity in the membrane matrix leads to a loose
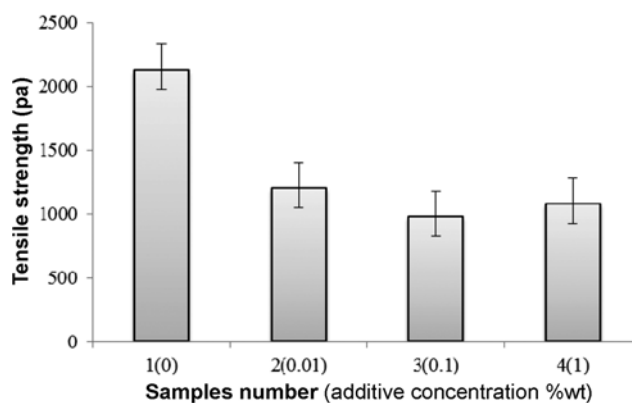

Fig. 11. The effect of PANI-co-MWCNT nanoparticle concentration on membrane tensile strength.

structure for the membranes [40]. In this case, the breaking point for membranes versus of tension force is reduced. To minimize the experimental errors, all measurements were carried out three times and then their average was reported.

6. 3D Surface Image

3D surface images showing the surface roughness of prepared membranes are presented in Fig. 12, where the convex parts of pure PES membrane are sharp, leading to higher hydrophobic
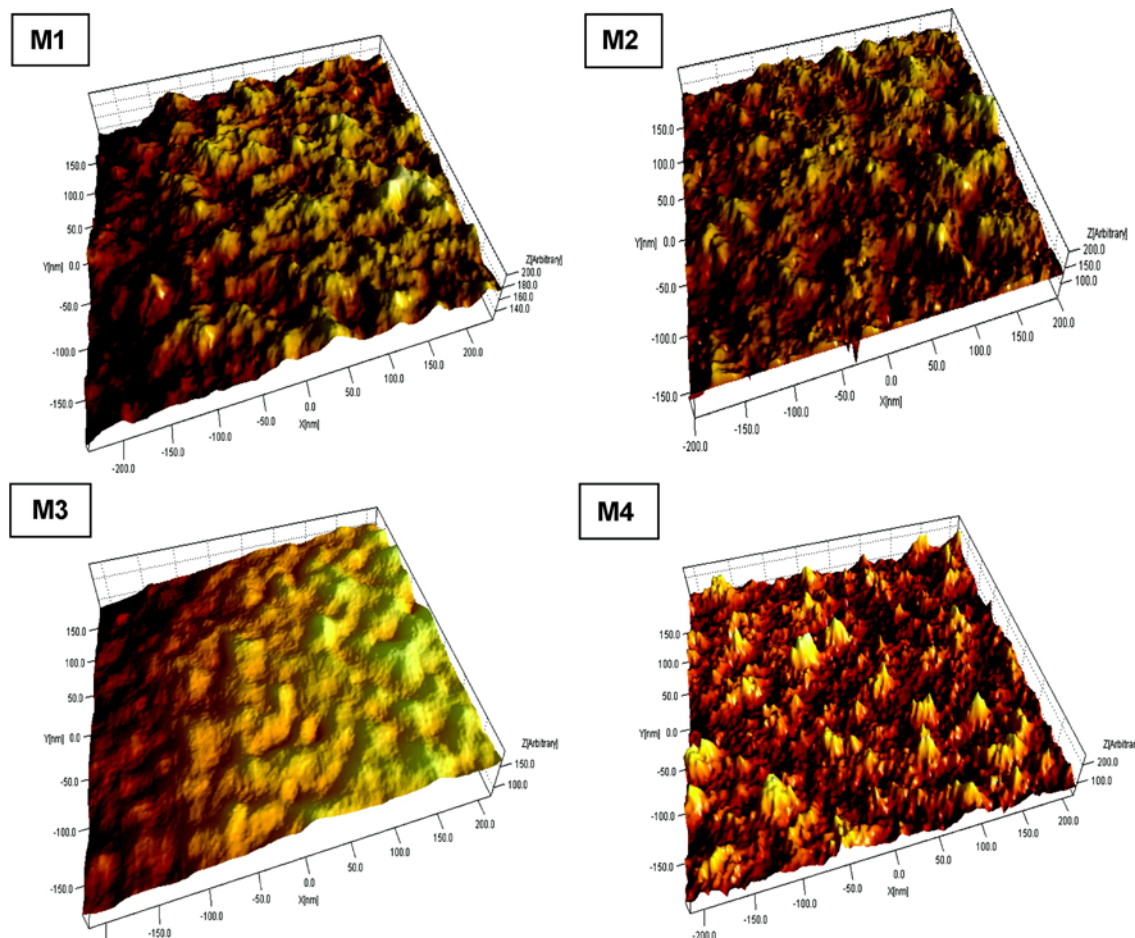

Fig. 12. 3D surface images of prepared membranes with various PANI-co-MWCNT nanoparticles concentration.

characteristic of the membrane surface (see Fig. 6). As shown, the mixed matrix membranes (M2 and M3) embedded with PANI-co-MWCNT nanoparticles are obviously smoother than that of the unfilled PES membrane. After addition of PANI-co-MWCNT nanoparticles (with the loading ratio of 0.1 wt%) into casting solution, membrane surface morphology (M3) is obviously changed and the convex areas become much smoother, which can introduce more hydrophilic characteristic of the mixed matrix membrane (PES/PANI-co-MWCNT). With the low content of nanoparticles loaded into the membrane matrix, due to the low interfacial interactions, more uniform/regular dispersion of them into the membrane matrix will be achieved, which can make the membrane surface smoother [45].

As can be seen in this figure, the roughness of prepared mixed matrix membrane embedded with high PANI-co-MWCNT nanoparticle content (M4), clearly increased compared to M3, which can be related to excessive nanoparticle content located on the membrane surface, leading to higher convex areas and roughness.

The modified nanofiltration membrane containing 0.1%wt PANI-co-MWCNTs composite nanoparticles showed better performance in terms of salt rejection and water flux compared to other prepared membranes.

CONCLUSION

Novel PES/PANI-co-MWCNT nanocomposite membrane was prepared by casting solution technique and phase inversion method. The effect of PANI-co-MWCNT nanoparticle concentration in casting solution on membrane properties and performance was studied. Scanning optical microscopy (SOM) and scanning electron microscopy (SEM), FTIR analysis, porosity and mean pore size, contact angle, water content, NaCl/Na$_2$SO$_4$ rejection, water flux and tensile strength measurements were also carried out in membrane characterization. The FTIR spectrum approved presence of PANI-co-MWCNT in the mixed matrix. It was found that utilization of PANI-co-MWCNT nanoparticles in the casting solution generally caused an increase in porosity, pore size, contact angle and water content. Just a little reduction was seen in 1%wt nanoparticle addition in the membrane matrix. The salt rejection and water flux were improved initially by an increase of nanoparticle concentration up to 0.1%wt in the membrane matrix and then decreased by more additive content. SOM images also showed nanoparticle agglomeration in membrane matrix at high additive loading ratio. Mechanical strength of prepared membrane declined by use of PANI-co-MWCNTs composite nanoparticles. After the addition of PANI-co-MWCNTs composite nanoparticles into casting solution, the membrane surface morphology was obviously changed and very much smoother surface was observed. Among the prepared membranes, composite membrane containing 0.1%wt PANI-co-MWCNTs composite NPs showed better performance compared to other modified membranes and also unmodified ones.

ACKNOWLEDGEMENT

REFERENCES

1. L. F. Greenlee, D. F. Lawler, B. D. Freeman, B. Marrot and P. Moulin, *Water Res.*, **43**, 2317 (2009).
2. B. J. A. Tarboush, D. Ranaa, T. Matsuura, H. A. Arafat and R. M. Narbaitz, *J. Membr. Sci.*, **325**, 166 (2008).
3. Y. Song, F. Liu and B. Sun, *J. Appl. Polym. Sci.*, **95**, 1251 (2005).
4. C. H. Cho, K. Y. Oh, S. K. Kim, J. G. Yeo and P. Sharma, *J. Membr. Sci.*, **371**, 226 (2011).
5. P. Eriksson, *J. Membr. Sci.*, **36**, 297 (1988).
6. A. E. Simpson, C. A. Kerr and C. A. Buckley, *Desalination*, **64**, 305 (1987).
7. J. E. Cadotte, F. Forester, M. Kim, R. J. Petersen and T. Stocker, *Desalination*, **70**, 77 (1988).
8. L. P. Raman, M. Cheryan and N. Rajagopalan, *Chem. Eng. Prog.*, **90**, 68 (1994).
9. R. J. Petersen, *J. Membr. Sci.*, **83**, 81 (1993).
10. R. Du and J. Zhao, *J. Membr. Sci.*, **239**, 183 (2004).
11. M. Mulder, *Basic Principles of Membrane Technology*, Kluwer Academic Publishers, Dordrecht (1997).
12. N. Ghaemi, S. S. Madaeni, A. Alizadeh, P. Daraei, V. Vatanpour and M. Falsafi, *Desalination*, **290**, 99 (2012).
13. R. E. Kesting, *Synthetic Polymeric Membranes*, Wiley, New York (1985).
14. N. Maximous, G. Nakhla, W. Wan and K. Wong, *J. Membr. Sci.*, **341**, 67 (2009).
15. F. Liu, N. A. Hashim, Y. Liu, M. R. Moghareh Abed and K. Li, *J. Membr. Sci.*, **375**, 1 (2011).
16. A. R. Khodabakhshi, S. S. Madaeni and S. M. Hosseini, *Polym. Int.*, **60**, 466 (2011).
17. A. Zendehnam, M. Arabzadegan, S. M. Hosseini, N. Robatmili and S. S. Madaeni, *Korean J. Chem. Eng.*, **30**(6), 1265 (2013).
18. A. Zendehnam, M. Rabieyan, S. M. Hosseini and S. Mokhtari, *Korean J. Chem. Eng.*, **32**(3), 501 (2015).
19. M. Kogure, H. Ohya, R. Paterson, M. Hosaka, J. Kim and S. Mc Fadzean, *J. Membr. Sci.*, **126**, 161 (1997).
20. H. Ohya, K. Masaoka, M. Aihara and Y. Negishi, *J. Membr. Sci.*, **146**, 9 (1998).
21. J. M. Thomassin, J. Kollar, G. Caldarella, A. Germain, R. Jerome and C. Detrembleur, *J. Membr. Sci.*, **303**, 252 (2007).
22. R. E. Sabzi, K. Rezapour and N. Samadi, *J. Serb. Chem. Soc.*, **75**(4), 537 (2010).
23. G. Wang, Y. Ding, F. Wang, X. Li and C. Li, *J. Colloid Interface Sci.*, **317**, 199 (2008).
24. M. S. Mansour, M. E. Ossman and H. A. Farag, *Desalination*, **272**, 301 (2011).
25. A. A. Khan and L. Paquiza, *Desalination*, **265**, 242 (2011).
26. P. Liu, *Eur. Polym. J.*, **41**, 2693 (2005).
27. P. Daraei, S. S. Madaeni, N. Ghaemi, H. Ahmadi Monfared and M. A. Khadivi, *Sep. Purfi. Technol.*, **104**, 32 (2013).
28. C. Oueiny, S. Berlioz and F. X. Perrin, *Prog. Polym. Sci.* (2014), http://dx.doi.org/10.1016/j.progpolymsci.2013.08.009.
29. X. Li, Z. Wang, H. Lu, C. Zhao, H. Na and C. Zhao, *J. Membr. Sci.*, **254**, 147 (2005).
30. S. M. Hosseini, A. R. Hamidi, S. S. Madaeni and A. R. Moghadassi, *Korean J. Chem. Eng.*, **32**(3), 429 (2015).

31. V. Vatanpour, S. S. Madaeni, R. Moradian, S. Zinadini and B. Astinchap, *Sep. Purfi. Technol.*, **90**, 69 (2012).
32. N. A. A. Hamid, A. F. Ismail, T. Matsuura, A. W. Zularisam, W. J. Lau, E. Yuliwati and M. S. Abdullah, *Desalination*, **273**, 85 (2011).
33. B. Van der Bruggen, *J. Appl. Polym. Sci.*, **114**, 630 (2009).
34. M. K. Mandal, S. Dutta and P. K. Bhattacharya, *Chem. Eng. J.*, **138**, 10 (2008).
35. R. Han, S. Zhang, C. Liu, Y. Wang and X. Jian, *J. Membr. Sci.*, **345**, 5 (2009).
36. A. Gholami, A. R. Moghadassi, S. M. Hosseini, S. Shabani and F. Gholami, *J. Ind. Eng. Chem.*, **20**, 1517 (2014).
37. N. Ghaemi, S. S. Madaeni, P. Daraei, H. Rajabi, T. Shojaeimehr, F. Rahimpour and B. Shirvani, *J. Hazard. Mater.*, **298**, 111 (2015).
38. V. Vatanpour, S. S. Madaeni, R. Moradian, S. Zinadini and B. Astinchap, *J. Membr. Sci.*, **375**, 284 (2011).
39. S. Ansari, A. R. Moghadassi and S. M. Hosseini, *Desalination*, **357**, 189 (2015).
40. S. M. Hosseini, F. Jeddi, M. Nemati, S. S. Madaeni and A. R. Moghadassi, *Desalination*, **341**, 107 (2014).
41. P. Le-Clech, V. Chen and T. A. G. Fane, *J. Membr. Sci.*, **284**, 17 (2006).
42. D. Rana and T. Matsuura, *Chem. Rev.*, **110**, 2448 (2010).
43. P. Daraei, S. S. Madaeni, N. Ghaemi, E. Salehi, M. A. Khadivi, R. Moradian and B. Astinchap, *J. Membr. Sci.*, **415**, 250 (2012).
44. P. Mobarakabad, A. R. Moghadassi and S. M. Hosseini, *Desalination*, **365**, 227 (2015).
45. S. Qiu, L. Wu, X. Pan, L. Zhang, H. Chen and C. Gao, *J. Membr. Sci.*, **342**, 165 (2009).